An accessible patient-derived xenograft model of low-risk myelodysplastic syndromes

Myelodysplastic syndromes (MDS) are among the most common myeloid malignancies.[1] They encompass a spectrum of clonal bone marrow (BM) failure diseases characterized by ineffective hematopoiesis and progression to acute myeloid leukemia (AML).[2] The clinical course of MDS varies widely from indolent, requiring only monitoring/supportive care, to aggressive disease with AML-like biology.[1] Recurrent somatic mutations contribute to the pathophysiology, being recently incorporated into prognostic scoring systems.[2,3] Akin to targeted therapy in AML, somatic mutations might be therapeutically targeted in MDS. Unfortunately, testing this hypothesis has been challenging due to the lack of preclinical models that truly recapitulate disease biology, particularly in lower-risk disease. This limitation has resulted in a dearth of novel targeted therapeutics and slow drug development in the field.[4]

Genetically engineered mouse models of recurrent somatic mutations present in MDS hold promise for advances in understanding the biology of these diseases. However, given that introns are generally not conserved between mice and humans, there is potential for significant differences in intron retention and cryptic splicing between human and mouse hematopoietic cells bearing spliceosome mutations.[4] The lack of readily available patient-derived xenograft (PDX) models remains the major barrier to drug development. NSG/NSG-S mice lack functional B, T, and natural killer cells as well as immunoglobulins,[5] and are unreliable for establishing PDX of low-risk MDS.[4] Our previous experience with conditioning regimens based exclusively on radiotherapy did not result in engraftment of MDS cells (*data not shown*). Recently, PDX models of MDS based on intra-bone co-injection of human mesenchymal stromal cells[6] or subcutaneous generation of ossicles using human mesenchymal stromal cells[7] have mitigated this shortcoming. Moreover, intra-hepatic injection of OKT3-depleted MDS BM into double-irradiated newborn MISTRG mice resulted in robust and reliable engraftment.[8] However, these models are not widely available and require technical skills that reduce their utility. It would, therefore, be opportune to develop a PDX model that is more suitable for testing novel targeted therapies and that allows for high throughput drug screening in low-risk diseases.

MISTRG mice are similar to other xenograft models in the sense that they are immunocompromised and express human cytokines (knocked-in in the case of MISTRG mice). Nevertheless, one key feature of MISRTG mice is their expression of human SIRPα. Their ability to recognize human CD47 (the “don’t eat me” signal) may explain the more reliable engraftment of human cells in these mice.[9] One way to reproduce this feature in NSG/NSG-S mice is by depleting macrophages with clodronate. Intraperitoneal administration of 100 μL of clodronate liposomes (FormuMax) to 6- to 8-week-old mice (NOD.*Cg-Prkdc*^{scid}*Il2rg*^{tm1Wjl}/NSG-Tg(CMV-IL3,CSF2,KITLG)1Eav/MloySzJ-NSG-S, prior to Jackson Laboratories; Jackson Laboratories), led to an 83% reduction of macrophages in the BM, and >99% reduction in the spleen after 48 h (*Online Supplementary Figure S1A, B*). The depletion persisted 7 days later, with 97% reduction in the BM, and still >99% in the spleen (*Online Supplementary Figure S1A, B*). In contrast, administration of 2 Gy of radiotherapy (classically used for conditioning) did not affect the presence of macrophages in the BM or spleen (*Online Supplementary Figure S1A, B*). To test whether depletion of macrophages enabled engraftment of patient-derived MDS cells, we conditioned 6- to 8-week-old NSG/NSG-S mice with 100 μL of clodronate liposomes, on day -2 and irradiated them with 2 Gy on day 0. Six hours later, we injected CD34$^+$ cells, via the tail vein; the cells were selected, as previously published,[7] from the BM of a patient with low-risk MDS (Figure 1A). At the time of sample collection, the patient had 1-2% CD34$^+$ blasts (Table 1). The BM samples came from MDS patients who had consented to participate in this study in accordance with the Declaration of Helsinki. The research protocol was approved by the Johns Hopkins Institutional Review Board. Flow-cytometry analysis of peripheral blood collected from transplanted mice 1, 2, and 3 months after transplantation showed the presence of human leukocytes (mouse CD45$^-$[mCD45$^-$] human CD45$^+$[hCD45$^+$]) (Figure 1B). At 3 months after transplantation, NSG mice showed reliable engraftment in the BM (*Online Supplementary Figure S1C*). NSG-S mice demonstrated consistent engraftment in the peripheral blood, spleen, and BM (*Online Supplementary Figure S1C, Table 1*). Furthermore, NSG-S mice showed detectable CD34$^+$ leukocytes (mCD45$^-$hCD45$^+$hCD34$^+$) as well as human erythroid cells (mCD45$^-$hCD45$^-$glycophorin A$^+$ [GPA$^+$]) in the BM at 3 months after transplantation. Using hCD45 beads and a magnetic column (Miltenyi), we selected hCD45$^+$ cells from the BM of these mice. hCD45$^+$ cells were pooled together and DNA was extracted using the Quick-DNA Miniprep Plus kit (Zymo Research). Libraries were prepared using a xGen Prism DNA Library Prep Kit (IDT) and IDT hybridization capture-based targeted duplex sequencing was done on a NOVASeq6000 platform in an SP flow cell. Data analyzed using DRAGEN Enrichment (v4.0.3) showed

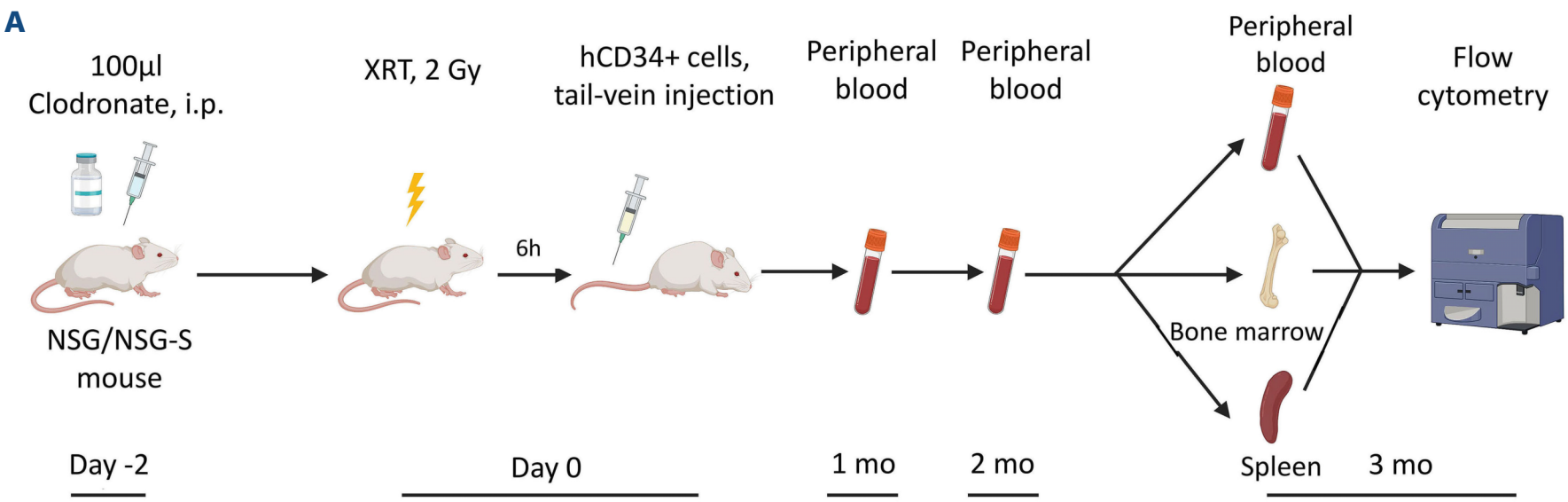

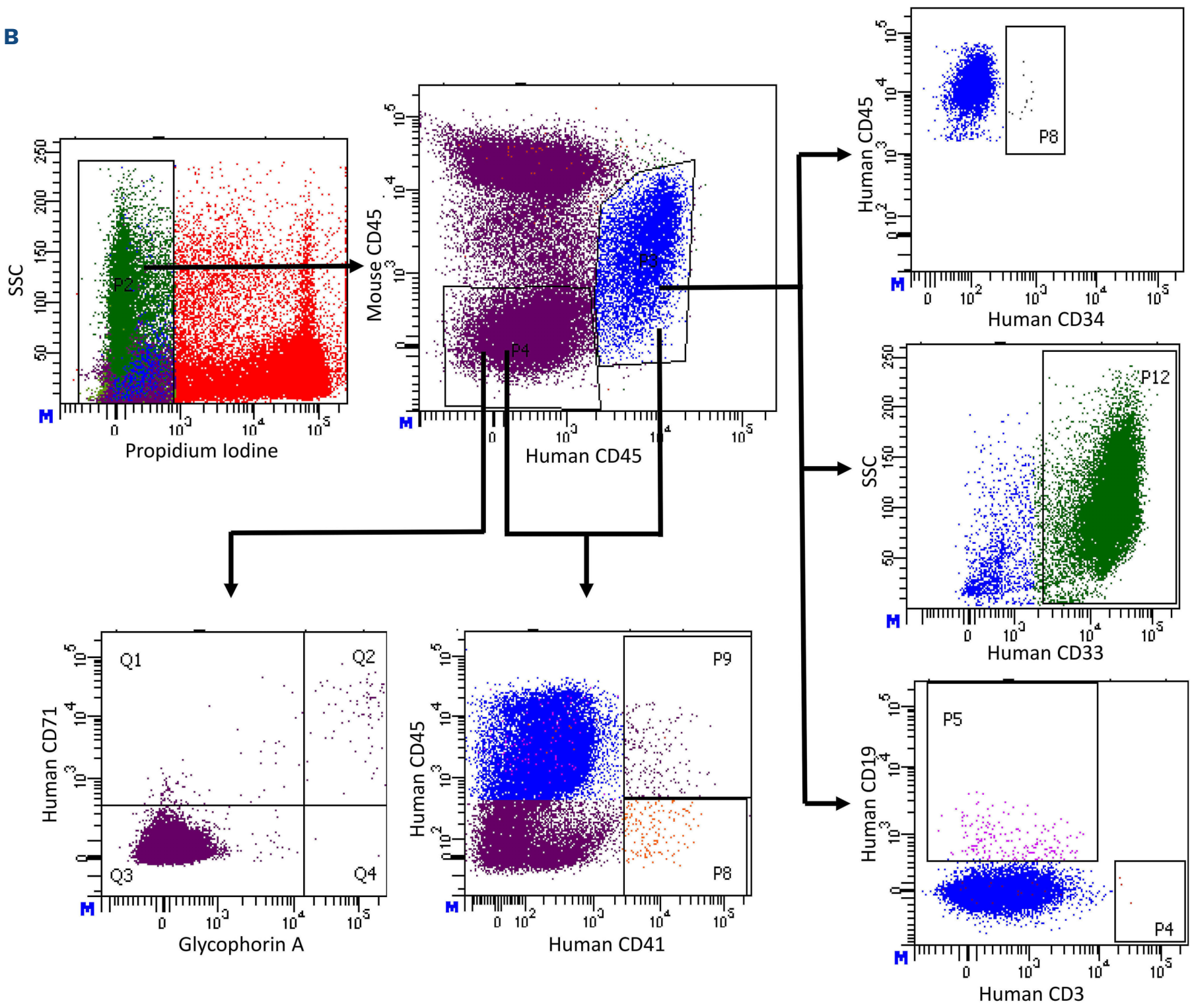

Figure 1. Clodronate and radiotherapy conditioning allow for reconstitution of human low-risk myelodysplastic syndrome hematopoiesis in NSG-S mice. (A) Graphic representation of the mouse engraftment technique and assessment. (B) Representative flow cytometry analysis of the human graft in an NSG-S mouse. Data were analyzed using BD FACSDiva software v8.0.1. i.p.: intraperitoneal; XRT: radiotherapy; mo: months; SSC: side scatter.

Table 1. Engraftment of primary low-risk myelodysplastic syndrome samples into NSG-S mice, after macrophage depletion, is reliable regardless of the cytogenetics or type of sample used. The table shows the patients' characteristics for the samples used for engraftment (top) and human cell populations and percentages in the peripheral blood (at different timepoints), bone marrow and spleen of NSG-S mice (bottom).

Sample	Age in years	NGS data for patients' clinical samples			Karyotype	BM blasts, %	Hemoglobin, g/dL	Platelets, x10^9/L	ANC, x10^9/L	IPSS-R score/category	IPSS-M score/category
		Gene	AA change	VAF							
Patient 1	74	*U2AF1*	p.S34F	41.1	47,XY+8[4]/ 46, XY[17]	<2%	9.4	338	2.45	3 points/low risk	0.23/moderate high risk
		ASXL1	p.G646fs	5.8							
		ASXL1	p.F1005fs	26							
		NOTCH1	p.R955H	46.2							
		NRAS	p.A91G	41.7							
		NUP98	p.D1214N	47							
		PLCG2	p.T620M	48.9							
Patient 2	64	*SF3B1*	p.K700E	36.1	46, XY	<2%	12.4	299	1.36	1 point/very low risk	-2.3/very low risk
		KDM2B	p.T28fs	40.2							
		TET2	p.F683fs	26.7							
Patient 3	74	*ASXL1*	p.G646fs	27.7	46,XY	3%	8.8	88	1	3.5 points/intermediate risk	0.45/moderate high risk
		EZH2	p.K634N	51.2							
		PHF6	p.C28fs	20.4							
		TET2	p.Q1030fs	48.2							
		ZRSR2	p.V253	89.7							

Sample	Sample type	N of cells (N of mice)	Peripheral blood					Bone marrow – final									Spleen – final								
			% hCD45$^+$ mean±SD					% hCD45$^+$ mean±SD					hCD45$^-$mCD45$^-$ mean±SD				% hCD45$^+$ mean±SD					hCD45$^-$mCD45$^-$ mean±SD			
			1 mo	2 mo	3 mo	4.5 mo - D17 Aza1	5 mo - D44 Aza1	Total	CD41$^+$	CD20$^+$/ CD19$^+$	CD3$^+$	CD33$^+$	CD71$^+$	GPA$^+$	CD71$^+$ GPA$^+$	CD41$^+$	Total	CD41$^+$	CD20$^+$/ CD19$^+$	CD3$^+$	CD33$^+$	CD71$^+$	GPA$^+$	CD71$^+$ GPA$^+$	CD41$^+$
Patient 1	Fresh	2x10^6/ mouse (3)	10.4± 3.4	7.6	11.3	NA	NA	12.7± 3.38	NA	NA	NA	NA	NA	0.1	NA	NA	35.65± 27.22	NA	NA	NA	NA	NA	0	NA	NA
Patient 2	Fresh	75x10^3/ mouse (3)	14± 3.25	6.5± 0.64	9.9± 2.68	NA	NA	23.1± 4.35	0	0.11± 0.06	0.02± 0.01	90.7± 3.7	0.03± 0.01	0.05± 0.03	0.03± 0.04	0.03± 0.04	12.86± 1.65	0	1.28± 0.77	0	88.03 ± 4.7	0.01± 0	0.01± 0.005	0	0.02± 0.01
Patient 3	IPSS-R	100x10^3/ mouse (5)	7.9± 3.09	3.22± 1.13	2.28± 0.86	No Aza 2.56± 0.87	9.16± 9.99	96.83 ± 2.5	0.38± 0.37	0.57± 0.17	0	74.6± 2.93	26.5± 4.2	0	2.46± 3.27	0.63± 0.62	16.4± 12.93	0.47± 0.05	0.6± 0.1	0	38.2± 4.02	26.5± 4.2	0	0	0.17± 0.09
						Aza 8.25± 0.95	11.45± 12.51	55.4± 19.79	0.1± 0	2.1± 0.6	0	62.6± 19.6	4.45± 4.05	0	0.1± 0	0.1± 0	17.6± 6.92	0.45± 0.15	0.5± 0.1	0	48.7± 0.5	0.1± 0	0	0	0.25± 0.05

NGS: next-generation sequencing; AA: amino acids; VAF: variant allele frequency; BM: bone marrow; ANC: absolute neutrophil count; IPSS-R: Revised International Prognostic Scoring System; IPSS-M: Molecular International Prognostic Scoring System; SD: standard deviation; h: human; m: mouse; mo: months; NA: not available; Aza: azacitidine.

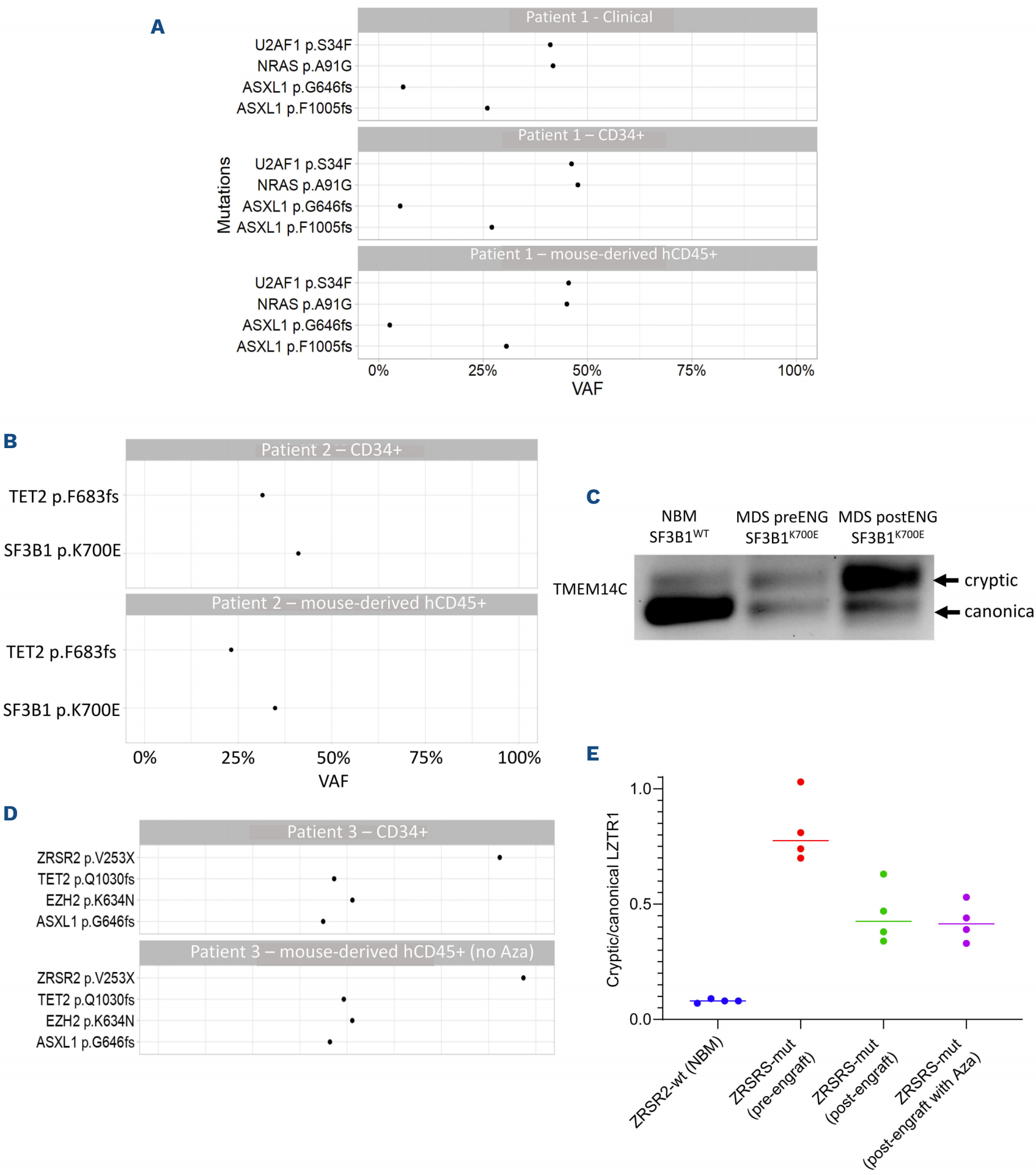

Figure 2. Engrafted low-risk myelodysplastic syndrome cells maintain the cytogenetics (and their functional impact) of the original patients' samples. (A) Comparison between the mutational profiles identified in the clinical report of patient 1 *versus* those in an analysis of CD34$^+$ cells sorted before transplantation and pooled human CD45$^+$ (hCD45$^+$) cells sorted from mouse bone marrow (BM) 3 months after transplantation. (B) Comparison between the mutational profiles in the CD34$^+$ cells sorted from patient 2 before transplantation and the pooled hCD45$^+$ cells isolated from the BM of mice engrafted with cells from patient 2, at 3 months after transplantation. (C) Splicing assay showing abnormal intron retention in the hCD45$^+$ cells of patient 2 prior to engraftment (MDS preENG, column 2) and those isolated from the BM of mice engrafted with cells from this patient at 3 months after transplantation (MDS postENG, column 3) as predicted in *SF3B1*-mutant cells. (D) Comparison between the mutational profile of CD34$^+$ cells sorted from patient 3 before transplantation and the pooled hCD45$^+$ cells sorted from the BM of mice engrafted with cells from patient 3 at 6 months after transplantation. (E) Ratio of cryptic (abnormal intron retention) to canonical *LTZR1* splicing in the pooled hCD45$^+$ cells isolated from the BM of mice engrafted with cells from patient 3 as predicted in *ZRSR1*-mutant cells. Each dot represents an independent experiment, horizontal lines represent the mean of four experiments. VAF: variant allele frequency; NBM: normal bone marrow; MDS: myelodysplastic syndrome; Aza: azacitidine.

that the selected hCD45$^+$ cells had a similar clonal architecture to that of the transplanted CD34$^+$ cells and the clinical samples (Figure 2A). Secondary transplantation using 10^6 hCD45$^+$ cells isolated from the BM of NSG/NSG-S mice resulted in detectable human engraftment, albeit at lower levels compared to those in primary recipients (*data not shown*).

We tested the reproducibility of the NSG-S model using various conditions: different CD34$^+$ numbers, fresh *versus* frozen cells and clinical specimens from low-risk MDS patients with different molecular profiles (Table 1). Human leukocytes were present in the peripheral blood of all mice at 1 (0.52%-14%) and 3 months (3.1%-20.7%) after transplantation (Table 1). Similarly, we observed successful engraftment in the BM (18.1%-99.3%) and spleen (8.1%-31.3%) at 3-6 months after transplantation (engraftment levels for each individual mouse are shown in *Online Supplementary Figure S1C*). Human cells were mostly CD33$^+$ myeloid cells (38.2%-90.7% of hCD45$^+$ cells). B-cell engraftment, as detected by the presence of CD19$^+$/CD20$^+$ cells (0.11%-2.1% of hCD45$^+$) was present in a subset of animals. No mice showed CD3$^+$ T- cell engraftment. Human erythroid engraftment is particularly difficult to achieve in xenograft models, as erythroid precursor cells are constantly removed by host macrophages. The depletion of macrophages with clodronate resulted in erythropoietic cell engraftment including hCD45$^-$hCD71$^+$ and hCD45$^-$hCD71$^+$GPA$^+$ cells in the BM and spleen of recipient mice (Figure 1B, Table 1). In addition, hCD45$^+$hCD41$^+$ (0.14%-0.47% of hCD45$^+$) and hCD45$^-$hCD41$^+$ (0.1%-0.63% of mCD45$^-$hCD45$^-$) megakaryocyte lineage cells were present in the BM and spleen.

The clonal architecture of engrafted cells recapitulated that of the clinical BM samples and enriched CD34$^+$ cells (Figure 2A, B, D). In lieu of morphological analysis of engrafted human cells, we investigated whether these cells showed preserved cryptic intron retention, similarly to the original sample. To this end, we extracted mRNA (from the pooled hCD45$^+$ cells sorted from the mouse BM) using the Monarch Total RNA Miniprep Kit and synthesized cDNA with the High-Capacity cDNA Reverse Transcription Kit in order to do splicing assays of the samples with mutated splicing factors (SF3B1 and ZRSR2). For the SF3B1 splicing assay, an isoform-competitive endpoint polymerase chain reaction for canonical cryptic acceptors in exon 2 of *TMEM14C* was performed with the primers GACACCTCGCAGTCATTCCT and TGATCCCACCAGAAGCAACC. For the ZRSR1 splicing assay, quantitative polymerase chain reaction was performed using the KAPA SYBR FAST qPCR Master Mix (2X) Kit with the primers CCCGCTCCAGCTACTTTGAA and CAAACAAGTAGAGCGAGTCCT for canonical *LZTR1* and primers CCCGCTCCAGCTACTTTGAA and AGTTCACTGGGGAGTGAGGAT for *LZTR1* intron 18 retention. The expression ratio was calculated with 2^-(canonical cycle threshold–cryptic cycle threshold). mRNA analysis of engrafted MDS cells with *SF3B1* (patient 2) and *ZRSR2* (patient 3) mutations validated the persistence of physiologically impactful[10,11] mis-splicing events in *TMEM14C* and *LZTR1*, respectively (Figure 2C, E).

For further exploration of disease relevance, after confirming engraftment, PDX derived from patient 3 were treated with either azacitidine (5 daily injections of 5 mg/kg, 2 cycles, 4 weeks apart) or saline. PDX treated with azacitidine showed decreased levels of BM engraftment at 6 months after transplantation (4 weeks after the completion of the 2nd cycle) (Table 1). Although not definitive (because of the small number of mice), these results serve as proof of concept of the model's applicability to study therapeutic interventions.

Recent years have seen the emergence of new technologies for augmentation of murine modeling of MDS, including genetically engineered mouse models and innovative PDX models. The PDX model described here complements currently available analytic tools in MDS. It makes use of relatively inexpensive and widely available reagents (i.e., NSG-S mice, clodronate, and radiation) and engraftment is tracked via non-invasive methods. Given the simplicity of its workflow, with no need for other moving parts (e.g., timed pregnancies, pre-engraftment of other cell populations or bone fragments), the use of viably frozen CD34$^+$ cells and easy conditioning regimen followed by intravenous injection, this model is suitable for large-scale drug testing in low-grade MDS. Typically, 20-30 mL of BM aspirate from a low-grade MDS sample may be sufficient to generate 50-60 PDX mice. Such scaling allows for testing of single-agent regimens (e.g., spliceosome inhibitors) and combination therapies (e.g., with hypomethylating agents) thus informing early-stage clinical development.

Authors

Patric Teodorescu,[1,2] Sergiu Pasca,[1] Inyoung Choi,[1] Cynthia Shams,[1] W. Brian Dalton,[1] Lukasz P. Gondek,[1] Amy E. DeZern[1] and Gabriel Ghiaur[1]

[1]Sidney Kimmel Comprehensive Cancer Center, Johns Hopkins University School of Medicine, Baltimore, MD, USA and [2]Universitatea de Medicina si Farmacie "Iuliu Hatieganu", Cluj-Napoca, Romania

Correspondence:
G. GHIAUR - gghiaur1@jhmi.edu

https://doi.org/10.3324/haematol.2023.282967

Received: March 6, 2023.
Accepted: June 29, 2023.
Early view: July 6, 2023.

Disclosures

CG has received research support from Menarini Ricerche, Abbie, Inc. and serves on an advisory board for Syros, Inc. WBD has received research support from Abbvie, Inc.

Contributions

PT wrote the manuscript, performed research, and analyzed data. SP analyzed sequencing data. IC designed, performed and analyzed the intron retention experiments. SC performed library preparation for sequencing experiments. WBD designed, performed and analyzed the splicing experiments. LPG designed, performed and analyzed the sequencing experiments. AED contributed patients' samples. GG designed the project. All authors critically reviewed the manuscript.

Funding

The work was funded by R01 HL159306, and P01 CA225618, P30 CA006973ASH, Bridge Award (to GG), a Johns Hopkins Hematological Malignancy Bone Marrow Transplant Pilot Grant (to AED and GG), and NCI R01 CA253981 (to AED and GG).

Data-sharing statement

The essential data supporting our findings are present within the article and Online Supplementary Material. The corresponding author can, upon reasonable request, provide raw data and additional details. All shared data will be anonymized for privacy.

References

1. Zeidan AM, Shallis RM, Wang R, Davidoff A, Ma X. Epidemiology of myelodysplastic syndromes: why characterizing the beast is a prerequisite to taming it. Blood Rev. 2019;34:1-15.
2. Sperling AS, Gibson CJ, Ebert BL. The genetics of myelodysplastic syndrome: from clonal haematopoiesis to secondary leukaemia. Nat Rev Cancer. 2017;17(1):5-19.
3. Bernard E, Tuechler H, Greenberg PL, et al. Molecular International Prognostic Scoring System for myelodysplastic syndromes. NEJM Evidence. 2022;1(7).
4. Liu W, Teodorescu P, Halene S, Ghiaur G. The coming of age of preclinical models of MDS. Front Oncol. 2022;12:815037.
5. Shultz LD, Lyons BL, Burzenski LM, et al. Human lymphoid and myeloid cell development in NOD/LtSz-scid IL2R gamma null mice engrafted with mobilized human hemopoietic stem cells. J Immunol. 2005;174(10):6477-6489.
6. Medyouf H, Mossner M, Jann JC, et al. Myelodysplastic cells in patients reprogram mesenchymal stromal cells to establish a transplantable stem cell niche disease unit. Cell Stem Cell. 2014;14(6):824-837.
7. Altrock E, Sens-Albert C, Jann JC, et al. Humanized three-dimensional scaffold xenotransplantation models for myelodysplastic syndromes. Exp Hematol. 2022;107:38-50.
8. Song Y, Rongvaux A, Taylor A, et al. A highly efficient and faithful MDS patient-derived xenotransplantation model for pre-clinical studies. Nat Commun. 2019;10(1):366.
9. Rongvaux A, Willinger T, Martinek J, et al. Development and function of human innate immune cells in a humanized mouse model. Nat Biotechnol. 2014;32(4):364-372.
10. Clough CA, Pangallo J, Sarchi M, et al. Coordinated missplicing of TMEM14C and ABCB7 causes ring sideroblast formation in SF3B1-mutant myelodysplastic syndrome. Blood. 2022;139(13):2038-2049.
11. Inoue D, Polaski JT, Taylor J, et al. Minor intron retention drives clonal hematopoietic disorders and diverse cancer predisposition. Nat Genet. 2021;53(5):707-718.